Available online at www.sciencedirect.com
ScienceDirect
Chinese Journal of Aeronautics 23(2010) 274-282
Chinese Journal of Aeronautics
www.elsevier.com/locate/cja

# Design and Optimization of Press Bend Forming Path for Producing Aircraft Integral Panels with Compound Curvatures

Yan Yu*, Wan Min, Wang Haibo, Huang Lin

*School of Mechanical Engineering and Automation, Beijing University of Aeronautics and Astronautics, Beijing 100191, China*

Received 16 January 2009; accepted 2 July 2009

**Abstract**

In order to find out the optimal press bend forming path in fabricating aircraft integral panels, this article proposes a new method on the basis of the authors' previous work. It is composed of the finite element method (FEM) equivalent model, the surface curvature analysis, the artificial neural network response surface and the genetic algorithm. The method begins with analyzing the objective's shape curvature to determine the bending position. Then it optimizes the punch travel at each bending position by the following steps: (1) Establish a multi-step press bend forming FEM equivalent model, with which the FEM experiments designed with the Taguchi method are performed. (2) Construct a back-propagation (BP) neural network response surface with the data from the FEM experiments. (3) Use the genetic algorithm to optimize the neural network response surface as the objective function. Finally, this method is verified by press bending a complicated double-curvature grid-type stiffened panel and bears out its effectiveness and intrinsic worth in designing the press bend forming path.

*Keywords:* press bend forming path; equivalent model; surface curvature analysis; neural network response surface; genetic algorithms; optimization

## 1. Introduction

Integrally stiffened panels have found broad application in advanced aircraft thanks to their light weight and high stiffness. By "integrally stiffened" is meant skin and stringers are made integrally into a single structure[1]. However, their increased structural complexity, their requirement for high-precision shape and satisfactory mechanical properties have also made their fabrication a formidable challenge to the aircraft manufacturers. A great number of researchers have been dedicating themselves to producing long-life and low-cost wing- and fuselage-panels for aircraft.

As a traditional and hitherto widely used forming method for aircraft integral panels, the bending on a brake-press possesses many advantages, such as low tooling cost, short cycle time and adaptability to a variety of shapes[1]. Based on the three-point bending principle, the press bend forming process involves multiple bending steps with universal dies according to planned paths to generate a single or a compound curvature shape.

As a complicated multi-step process, the aforesaid press bend forming accompanies multiple times of bending and springback with obvious interactions between them. The critical factor that affects the final shape of the products is the bend forming path, which includes the bending position and the punch travel. To plan a proper path always proves a tough work depending more on the skills and operators' experiences than the theoretical instructions. This might lead to bad product repeatability and forming quality. Therefore, to optimize the bend forming path with finite element method (FEM) and other methods is urgently needed.

So far lots of researchers have made valuable contributions to the press bend forming of aircraft panels. J. S. Liu, et al.[2-3] carried out experimental and numerical simulation studies on press bend forming to analyze strain and stress distribution during the forming process[4], buckling and fracture of stiffeners[5], springbacks and effects of the bending position[6]—all are quite helpful in laying bare the forming process. Furthermore, in order to realize numerical control of the press bending process, they proposed some methods to determine the relationship between the punch travels and the arc heights[6-8] and established a self-adaptive incremental press bending knowledge base system[9]. Their study provides precious help to

*Corresponding author. Tel.: +86-10-82338613.
*E-mail address:* anneyan@126.com
Foundation item: Specialized Research Fund for the Doctoral Program of High Education of China (20091102110021)


doi: 10.1016/S1000-9361(09)60216-8

fabricate small mono-curvature integral panels. However, till now few attempts have been made to simulate or optimize the press bend forming process of large-size double-curvature aircraft integral panels. This article is, therefore, meant to solve this problem by putting forward a new method.

Based on the Darwinian principles of natural selection—survival of the fittest, a natural genetic phenomenon, the genetic algorithm (GA), as a selective searching method capable of optimizing functions with unknown dependence of design variables has been widely applied to solving many optimization problems[10]. It is able to make an efficient search after very large solution spaces at a cost of lighter computational work since it uses probabilistic transition rules instead of deterministic ones. GA is the most fit for the problems, in which a minor change might cause serious nonlinear behavior in the solution space[11]. Nevertheless, it always takes GA optimization based on FEM several weeks to run numerous times of FEM analytical computation, thus terribly wasting the labor and time[12].

The response surface methodology (RSM) as an optimization method uses approximations to the objective and constraint functions, which are based on functional evaluations at selected points in the design space[13]. By replacing the iterations of FEM analyses with the response surface, the efficiency can be remarkably enhanced. However, prediction based on the polynomial equation commonly used in RSM is often limited to low levels, resulting in poor estimations of optimal formulations[14]. Artificial neural network (ANN) has a considerable power to map the nonlinear relationship between inputs and outputs that cannot be efficiently predicted by analytical or conventional statistical models[15-16]. It has been proved that the neural network response surfaces are more precise than the polynomial response surfaces[17-22].

The goal of this article is to develop an approach associating objective's shape curvature analysis, FEM equivalent model[23], ANN and GA to attain an optimized path for press bend forming and present an example to verify the effectiveness of this new method.

## 2. Theoretical Background

### *2.1. BP neural network response surface*

Back-propagation (BP) network is short for the feed-forward BP multilayer network. The information flow is only allowed to be in one direction during the training process. First, the network receives some information signals through the input layer and the output produced by the first layer is fed subsequently into the second layer and so on. The errors are then propagated backward[11].

The network adjusts its parameters by learning and training the data samples. Since this decides the neural network's foreseeing performance, it is crucial to determine the proper range of data to be used for neural network training with a good method to design the experiment. Taguchi method fits the bill for it enables to yield the full information of all the factors by conducting the least experiments[24]. With this method, the time spent on calculation can be greatly reduced and the "over-learning" of the network can be avoided. Hence, this articel adopts the Taguchi experiment designing method in FEM simulations to gain the training data samples.

### *2.2. Genetic algorithm*

As a method used to solve both constrained and unconstrained optimization problems, GA is able to find the global optimization point and its results are more reliable than those of other common methods. Furthermore, it is good at optimizing the "Black Box" problem, such as the trained neural network.

GA uses three main types of rules at each step to create the next generation from the current population. By selection rules, the individuals called parents, which contribute to the population for the next generation, are selected. By crossover rules are combined two parents to form children for the next generation. By mutation rules random changes are applied to individual parents to generate children.

### *2.3. Equivalent model of press bend forming*

FEM analysis seems to be unapplicable in the study of press bend forming of integrally stiffened panels due to their structural complexity, the multi-step forming process and the limitations by the hardware. Consequently, Ref.[23] proposed an equivalent model to improve efficiency of simulations and optimizations.

A plastic plate-form equivalent model made of a virtual material is bend formed into the shape similar to that of the detailed model along the same bending path. The specific plastic characteristics of the virtual material are obtained through in-depth analysis of the bending and springback mechanics of the detailed model. The key equations to calculate the virtual material parameters are grounded upon two assumptions: 1) both models yield at the same punch travel and 2) both models possess the same outer radius after springback. FEM simulation results indicate that at the same punch travel, the error of equivalent model is less than 6% while the efficiency of FEM simulation increases by 80%[23]. So it becomes possible to plan the forming path at the cost of much less modeling and time than with the detailed models.

Fig.1 illustrates the flowchart for optimization of the forming path in press bend forming of aircraft integral panels.

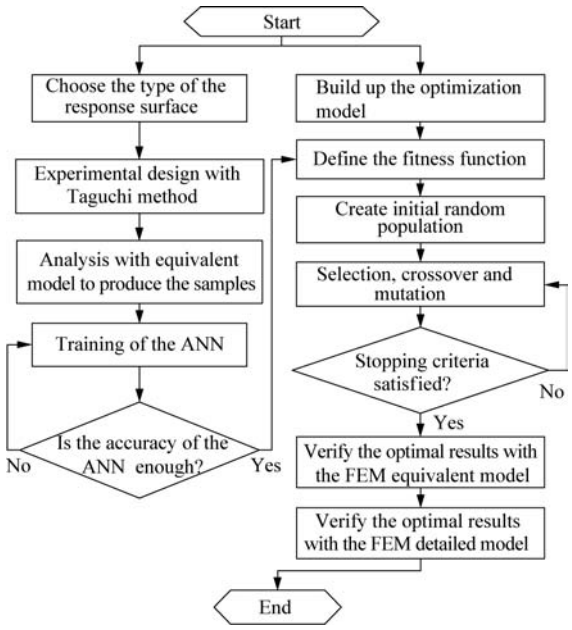


Fig.1 Flowchart for optimization of forming path based on BP-GA algorithm.

## 3. Design of Bending Position

### *3.1. Effects of bending position on shape of a formed panel*

To determine the bending position is the base of the forming path optimization, which also poses a real challenge to the process planning. In order to find out the effects of the bending position on the shape of the formed panel, FEM analysis is carried out to simulate a vertical bending and a sidelong bending of a small workpiece, as shown in Fig.2.

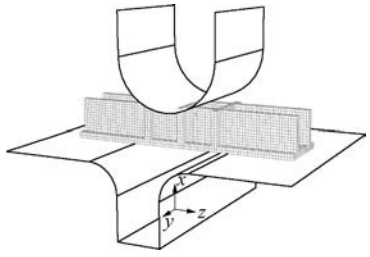

(a) Vertical bending

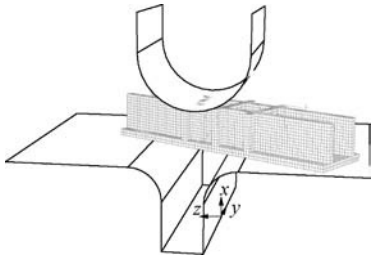

(b) Sidelong bending

Fig.2 FEM press bend forming model.

Neither node coordinates nor the displacements of the formed panel's outer surface could reflect the comprehensive effects of the bending position on the surface geometry, but the surface curvature could. As the curvature contour plots can well provide the information about the overall and local curvature distribution, the point clouds are extracted from the FEM results to reconstruct the surface and the curvature analysis is conducted with the CAD software. Fig.3 shows the curvature contour plots of workpieces formed at different bending positions. It can be seen that the surface curvature decreases gradually from the bending position to both sides. This finding is rather meaningful in determining the bending position.

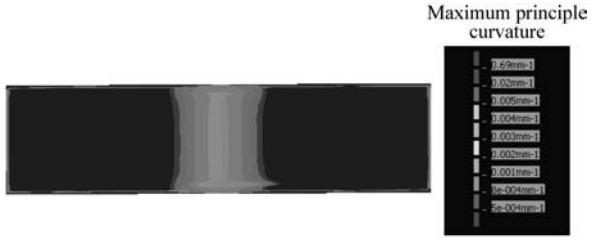


(a) Vertical bending


(b) Sidelong bending

Fig.3 Maximum principle curvature of skin outer surface after press bend forming.

### *3.2. Bending position design based on surface curvature analysis*

The double-curvature integral panel under investigation is designed. Unfold the double-curvature integral panel with CATIA V5R18, and let the dimensions of the unfolded panel be presented in Fig.4. From the afore said, it is understood that the objective's shape curvature should be analyzed before the bending position could be determined. The objective shape curvature of this integral panel is shown in Fig.5. It can be observed that the curvature distribution is quite regular. As the curvature decreases from the left to the right, obviously, the left part is more curved than the right.

From both the curvature distribution plot and the principles of press bend forming, it can be understood that the outer skin shape of the aircraft integral panel results from the accumulation of a great number of unparallel three-point bendings. Each region that possesses the similar curvature can be regarded as the effect of bending with the dies along its extension direction.

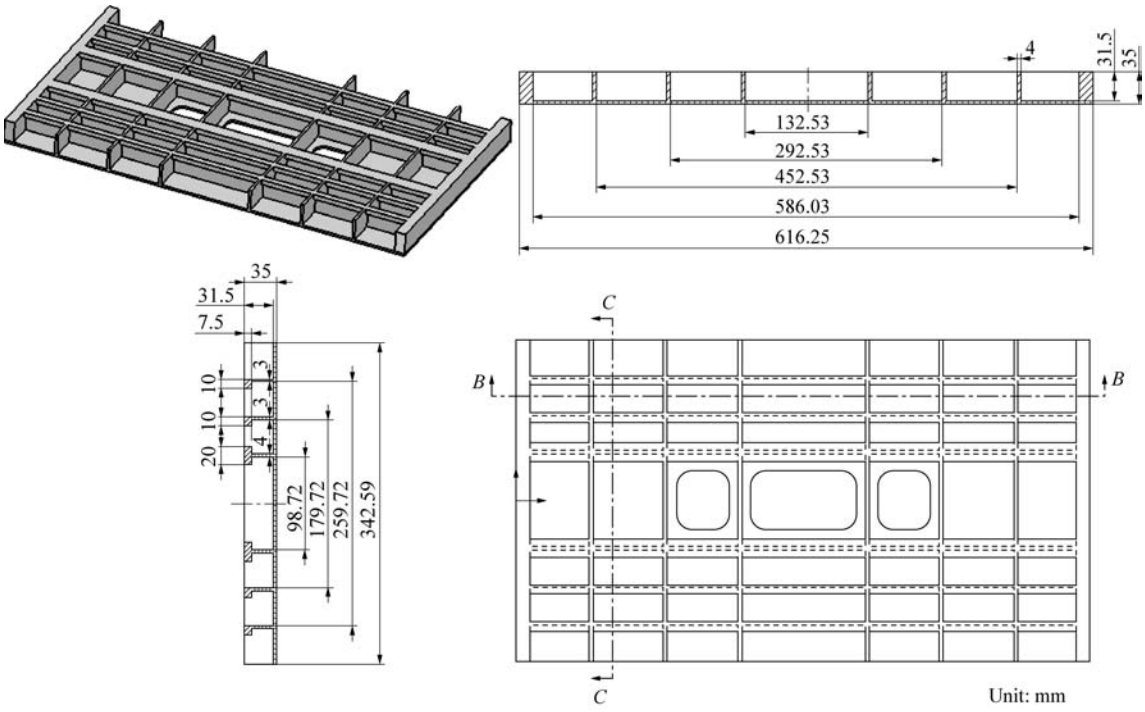


Fig.4 Structure of unfolded machined panel.

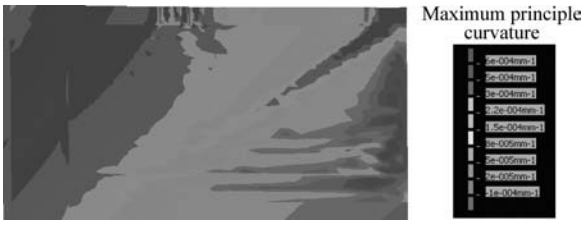


Fig.5 Maximum principle curvature of objective skin outer surface.

Based on the above analysis, the following procedure to determine bending positions can be put forward.

(1) Calculate the bending space with the dimensions of the dies.

Calculate the bending space without producing overlapped deformation through Eq.(1) with the dimensions (see Fig.6).

$$\Delta L' = D + 2R_D \tag{1}$$

where $\Delta L'$ is the bending space without producing overlapped deformation, $D$ the die gap, and $R_D$ the die radius.

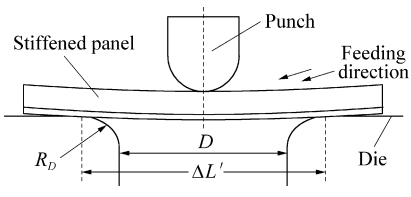


Fig.6 Sketch of bending space.

Without overlapped deformation, the formed panel would suffer from discontinued curvature and poor forming quality. From a number of numerical simulations, it comes to a conclusion that the amount of the overlapped deformation should not be less than $R_D$, and the continued curvature should be guaranteed. Therefore, the bending space can be determined by

$$\Delta L = D + R_D \tag{2}$$

where $\Delta L$ is the bending space when the amount of the overlapped deformation is $R_D$.

(2) Calculate the number of the bending steps in terms of the panel dimensions and the bending space (Eq.(3)).

$$n = \frac{L}{D + R_D} - 1 \tag{3}$$

where $L$ is the length of the panel diagonal or that of the side of the panel depending upon whether the main curvature changes along the diagonal or the side of the panel and $n$ the number of the bending steps.

(3) The bending position should be approximately located in the extension direction of the region with the similar curvature.

(4) Strive to distribute the actual bending spaces uniformly along the calculated $\Delta L$.

(5) Make sure the bending is applied to the sites as closely to the intersections of the stiffeners as possible.

(6) Prevent corners of the panel from slipping into the die.

Referring to the practices of aircraft manufacturers, the radius of the punch and the die under study is chosen to be 35 mm and the die gap 70 mm. Therefore,

the calculated bending space equals 105 mm and the number of bending positions is six. Fig.7 illustrates the bending positions according to the above-mentioned principles with the thick lines representing the bending positions.

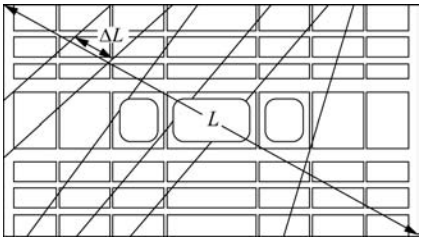


Fig.7 Sketch of press bending positions.

As a result, the method of designing press bend forming paths can be summarized as follows: first, determine the bending positions abiding by the above-instructed principles with the panel outer surface curvature distribution as the kernel factor; second, optimize the punch travel at each position with the proposed optimization algorithm.

## 4. Optimization of Punch Travels

### *4.1. Description of optimization problems*

(1) Objective function

Subtract point clouds from the skin outer surface of the formed panel and compare them with the discrete objective surfaces. Take the forming errors as the objective function of the optimization problem defined as

$$e_{\text{shape}} = |e_{\max}| + |e_{\min}| \tag{3}$$

where $e_{\max}$ and $e_{\min}$ are the maximum and the minimum error of the two aligned point clouds, respectively (see Fig.8).

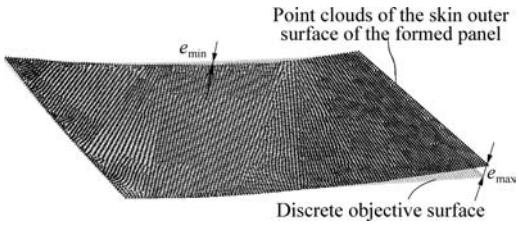


Fig.8 Sketch of maximum and minimum error.

(2) Design variables

Assume that $X_1$, $X_2$, $X_3$, $X_4$, $X_5$ and $X_6$ as the design variables of this optimization problem are the punch travels at six bending positions from the left to the right.

(3) Constraints

The punch travels commonly adopted in factories are around 5 mm due to the possibility of starting to appear bucklings on the stiffeners. Thus the punch travel less than 5 mm is set to be the constraint of the design variables.

### *4.2. FEM modeling of multi-step press bend forming*

The simulations are carried out with the commercial code ABAQUS. Press bend forming is a multi-step forming process and springbacks take place continually. In order to improve the simulation accuracy and avoid frequent alternative runs of the explicit and the implicit algorithms, both the forming and springback processes are simulated with the implicit algorithm. The workpiece is modeled with solid elements of C3D8R. The enhanced hourglass control approach is chosen. The tools are modeled with discrete rigid surfaces. The material is aluminum alloy 7B04-T7451. Fig.9 shows the assembled model in detail. By moving the punch and dies, press bending and springback at different positions are effectuated. The movements of the punch and dies are calculated based on the geometrical relationship between bending positions and panel outlines.

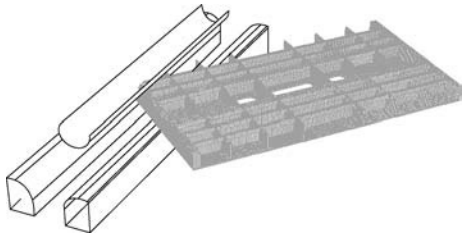

Fig.9 FEM detailed assembled model for press bend forming.

In order to enhance the calculation efficiency, an FEM equivalent model for press bend forming of integrally stiffened panels is established. The material parameters of the plastic equivalent plate-model are calculated with the method proposed in Ref.[23]. As the cross-sections of different bend lines have different shapes and dimensions, the virtual materials should be calculated accordingly. Table 1 lists the yield and hardening parameters of the six different virtual materials, which are used as the material data during FEM analysis. Fig.10 relates the six virtual materials accordingly to the positions of the panel, where the thick lines represent the six bend positions.

**Table 1 Material properties of virtual materials of equivalent model**

| Material | Elastic modulus $E$/GPa | Poisson ratio $\nu$ | Initial yield stress $\sigma_{sE}$/MPa | Hardening exponent $n_E$ | Hardening coefficient $K_E$ |
|---|---|---|---|---|---|
| 1 | 69 | 0.33 | 399.08 | 0.85 | 1 817.66 |
| 2 | 69 | 0.33 | 365.82 | 0.81 | 1 817.66 |
| 3 | 69 | 0.33 | 370.86 | 0.82 | 1 817.66 |
| 4 | 69 | 0.33 | 371.03 | 0.82 | 1 817.66 |
| 5 | 69 | 0.33 | 375.85 | 0.83 | 1 817.66 |
| 6 | 69 | 0.33 | 361.59 | 0.81 | 1 817.66 |

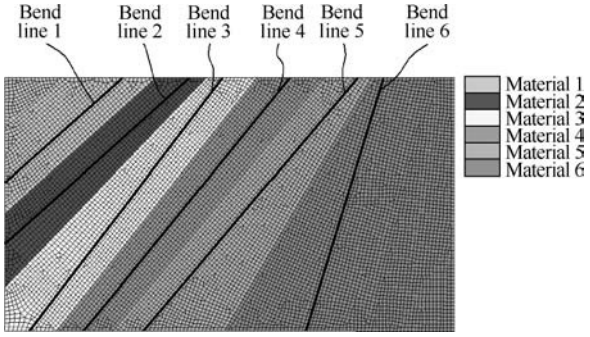


Fig.10 Virtual material's distribution of an FEM equivalent model.

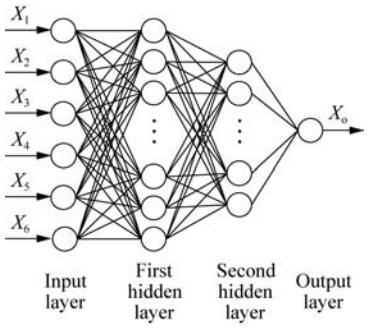


Fig.11 Topological structure of a BP neural network.

### *4.3. Establishment of neural network response surfaces*

The neural network response surface requires training by using the FEM experimental data based on equivalent model to map the relationships between the punch travels and the forming errors. The orthogonal $L_{25}(5^6)$ test matrix is adopted to design the experiment. Assume the punch travels $X_1$, $X_2$, $X_3$, $X_4$, $X_5$ and $X_6$ as the six experiment factors and the forming error $e_{\text{shape}}$ defined in Eq.(3) as the objective of the experiment. Table 2 shows the factors and levels of the Taguchi method.

**Table 2 Layout of Taguchi experiment**

| Factor | Level | | | | |
|---|---|---|---|---|---|
| | 1 | 2 | 3 | 4 | 5 |
| First punch travel $X_1$ /mm | 2.0 | 2.5 | 3.0 | 3.5 | 4.0 |
| Second punch travel $X_2$ /mm | 2.0 | 2.5 | 3.0 | 3.5 | 4.0 |
| Third punch travel $X_3$/mm | 1.5 | 2.0 | 2.5 | 3.0 | 3.5 |
| Fourth punch travel $X_4$/mm | 1.5 | 2.0 | 2.5 | 3.0 | 3.5 |
| Fifth punch travel $X_5$/mm | 1.5 | 2.0 | 2.5 | 3.0 | 3.5 |
| Sixth punch travel $X_6$ /mm | 1.0 | 2.0 | 2.5 | 3.0 | 3.5 |

Select twenty datasets rationally to be the training samples and the other five datasets inclusive of No.2, No.7, No.14, No.19, and No.25 the testing samples. Training is accomplished by using the BP algorithm. Ten neurons are used in the first hidden layer and eight in the second (see Fig.11).

The developed neural network has a tan-sigmoid transfer function in the hidden layers and a linear transfer function in the output layer. The Levenberg-Marquardt (LM) algorithm avoids computing Hessian matrix when modifying the second-order training speed. As this algorithm proves the fastest method for training moderate-sized feedforward neural networks, the LM back-propagation algorithm is used here for training and the gradient descent with momentum weight and bias learning function (Learngdm for short) are used for learning. Learngdm calculates the weight change for a given neuron based upon the neuron's input and error, the weight (or bias), learning rate and momentum constant according to the gradient descent with momentum. Let MSE denote the network performance function, which measures the network's performance by the mean of squared errors.

$$\text{MSE} = \frac{1}{N}\sum_{i=1}^{N}(e_i)^2 = \frac{1}{N}\sum_{i=1}^{N}(t_i - a_i)^2 \tag{4}$$

where $N$ is the total number of training datasets, $t_i$ the training sample data and $a_i$ the output of the neural network.

After the neural network is trained, its accuracy should be examined against untrained inputs so as to specify the network's accuracy to predict the quality of certain process. The other five datasets that were not in training are used to test the network. Table 3 compares the outputs of the neural network with the Taguchi test results. Note that the datasets with asterisks are the testing datasets for the neural network while the others are the training datasets. It is observed that the relative errors for all the datasets are less than 11%, which means that the developed neural network is rather effective in mapping the relationship between the punch travels and the press bend forming errors $e_{\text{shape}}$. Therefore it stands to reason for this neural network to displace the time-consuming FEM simulations in the GA optimization process to enhance the efficiency.

**Table 3 Comparison between outputs of neural network and Taguchi test results**

| Test No. | Punch travel/mm | | | | | | Taguchi test $e_{\text{shape}}$/mm | Neural network output $e_{\text{shape}}$/mm | Relative error/% |
|---|---|---|---|---|---|---|---|---|---|
| | Step 1 | Step 2 | Step 3 | Step 4 | Step 5 | Step 6 | | | |
| 1 | 2.0 | 2.0 | 1.5 | 1.5 | 1.5 | 1.0 | 15.33 | 15.24 | 0.59 |
| 2* | 2.0 | 2.5 | 2.0 | 2.0 | 2.0 | 2.0 | 9.31 | 9.53 | 2.36 |

Continued

| Test No. | Punch travel/mm | | | | | | Taguchi test $e_{shape}$/mm | Neural network output $e_{shape}$/mm | Relative error/% |
|---|---|---|---|---|---|---|---|---|---|
| | Step 1 | Step 2 | Step 3 | Step 4 | Step 5 | Step 6 | | | |
| 3 | 2.0 | 3.0 | 2.5 | 2.5 | 2.5 | 2.5 | 7.80 | 7.65 | 1.92 |
| 4 | 2.0 | 3.5 | 3.0 | 3.0 | 3.0 | 3.0 | 14.92 | 15.06 | 0.94 |
| 5 | 2.0 | 4.0 | 3.5 | 3.5 | 3.5 | 3.5 | 23.30 | 22.88 | 1.80 |
| 6 | 2.5 | 2.0 | 2.0 | 2.5 | 3.0 | 3.5 | 12.70 | 13.41 | 5.59 |
| 7* | 2.5 | 2.5 | 2.5 | 3.0 | 3.5 | 1.0 | 7.60 | 8.18 | 7.58 |
| 8 | 2.5 | 3.0 | 3.0 | 3.5 | 1.5 | 2.0 | 7.92 | 7.93 | 0.13 |
| 9 | 2.5 | 3.5 | 3.5 | 1.5 | 2.0 | 2.5 | 6.41 | 6.12 | 4.52 |
| 10 | 2.5 | 4.0 | 1.5 | 2.0 | 2.5 | 3.0 | 8.28 | 8.19 | 1.09 |
| 11 | 3.0 | 2.0 | 2.5 | 3.5 | 2.0 | 3.0 | 9.20 | 8.78 | 4.57 |
| 12 | 3.0 | 2.5 | 3.0 | 1.5 | 2.5 | 3.5 | 11.17 | 11.26 | 0.81 |
| 13 | 3.0 | 3.0 | 3.5 | 2.0 | 3.0 | 1.0 | 7.00 | 7.19 | 2.71 |
| 14* | 3.0 | 3.5 | 1.5 | 2.5 | 3.5 | 2.0 | 8.70 | 7.81 | 10.23 |
| 15 | 3.0 | 4.0 | 2.0 | 3.0 | 1.5 | 2.5 | 6.28 | 6.37 | 1.43 |
| 16 | 3.5 | 2.0 | 3.0 | 2.0 | 3.5 | 2.5 | 10.94 | 9.91 | 9.41 |
| 17 | 3.5 | 2.5 | 3.5 | 2.5 | 1.5 | 3.0 | 8.11 | 8.25 | 1.73 |
| 18 | 3.5 | 3.0 | 1.5 | 3.0 | 2.0 | 3.5 | 11.00 | 10.81 | 1.73 |
| 19* | 3.5 | 3.5 | 2.0 | 3.5 | 2.5 | 1.0 | 8.30 | 8.59 | 3.49 |
| 20 | 3.5 | 4.0 | 2.5 | 1.5 | 3.0 | 2.0 | 7.17 | 6.64 | 7.39 |
| 21 | 4.0 | 2.0 | 3.5 | 3.0 | 2.5 | 2.0 | 9.93 | 9.48 | 4.53 |
| 22 | 4.0 | 2.5 | 1.5 | 3.5 | 3.0 | 2.5 | 11.01 | 11.09 | 0.73 |
| 23 | 4.0 | 3.0 | 2.0 | 1.5 | 3.5 | 3.0 | 9.84 | 9.62 | 2.24 |
| 24 | 4.0 | 3.5 | 2.5 | 2.0 | 1.5 | 3.5 | 9.76 | 10.25 | 5.02 |
| 25* | 4.0 | 4.0 | 3.0 | 2.5 | 2.0 | 1.0 | 9.70 | 10.36 | 6.80 |

### *4.4. Optimization with genetic algorithm*

The fitness function is used to convert the values of objective function into the corresponding fitness value. With the M-file describing the objective function, the trained neural network response surface is defined as the fitness function for the GA optimization. Rank scaling function, stochastic uniform selection function, elite count reproduction function and Gaussian mutation function are all adopted as the GA options. In this study, the size of the initial population is 30 and the crossover rate 0.8. The stopping criterion is met when $X_1$=3.5 mm, $X_2$=3.0 mm, $X_3$=2.8 mm, $X_4$=1.7 mm, $X_5$=2.3 mm, $X_6$=1.3 mm. The output of the neural network with this input is $e_{shape}$=4.06 mm.

## 5. FEM Verification of Optimized Press Bend Forming Path

Verification of the optimized press bend forming path is carried out with both the FEM equivalent model and the FEM detailed model. Fig.12 compares the two point clouds of the outer surfaces of the formed panel with the discrete objective shape surface.

Table 4 lists the forming errors of the detailed-model and of the equivalent model before and after optimization. From the simulation results of the FEM equivalent model, it is clear that the optimized path proves much better than any press bend forming path in the Taguchi tests. In addition, this optimized path also works well with the detailed model with the forming error $e_{shape}$ of only 3.10 mm (the sum of the

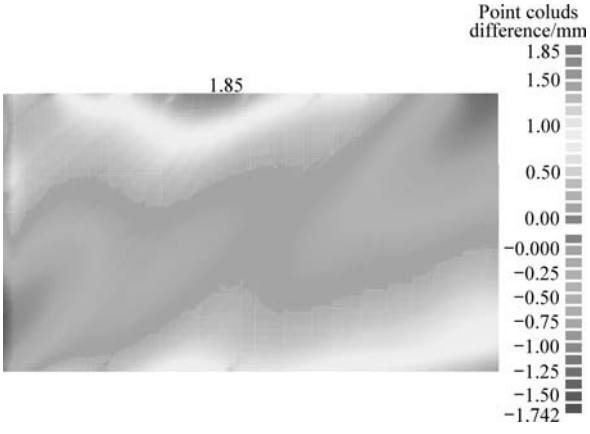


(a) FEM equivalent model results and objective shape surface

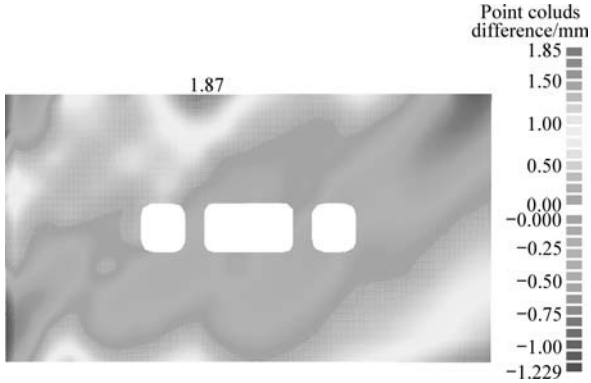


(b) FEM detailed model results and objective shape surface

Fig.12 Differences between formed outer skin surface and objective shape surface.

**Table 4 FEM verification of optimized bending path**

| Parameter | FEM equivalent model | FEM detailed model |
|---|---|---|
| Minimum $e_{shape}$ before optimization (Taguchi test)/mm | 6.28 | |
| Minimum $e_{shape}$ after optimization/mm | 3.59 | 3.10 |
| FEM analysis CPU time/($10^5$s) | 1.311 20 | 9.925 45 |

upper limit and the lower limit of the legend on the right of Fig.12(b)). The results indicate that the equivalent model performs quite well in the sense of "equivalent" and the calculation efficiency is up by 86.79%.

Fig.13 shows the equivalent plastic strain distribution of the detailed model formed in six-step bending procedure. It displays the stiffened panel having a smooth surface without any bucklings on the stiffeners, which evidences the ability of the optimized to ensure not only the shape accuracy but also the surface quality.

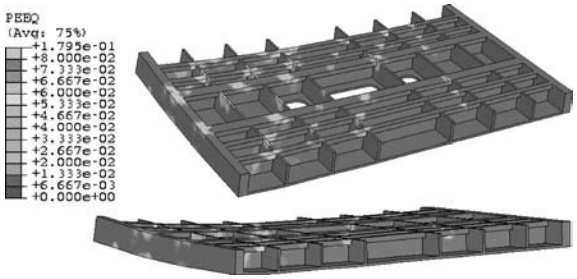


Fig.13 Equivalent plastic strain distribution of a detailed mode.

## 6. Conclusions

(1) The proposed method to determine bending positions based on the analysis of an objective's shape surface curvature proves of great effectiveness and convenience. It lays a good foundation for the optimization of punch travels at each bending position.

(2) The developed neural network response surface provides strong mapping ability and high precision for the press bend forming process in manufacturing aircraft integral panels. It succeeds in replacing the time-consuming FEM simulations in the GA optimization through much less runs of FEM calculation.

(3) The precise quantitative results of this study evince that the FEM equivalent model and neural network response surface associated with the GA can effectuate the fast optimization of the punch travels, a key problem in manufacturing aircraft integral panels. Furthermore, this study has paved the way for ulterior study of the optimization for other complicated forming processes.

## References

[1] Munroe J, Wilkins K, Gruber M. Integral airframe structures (IAS)—validated feasibility study of integrally stiffened metallic fuselage panels for reducing manufacturing costs. NASA/CR-2000-209337, 2000.

[2] Liu J S, Zhang S H, Wang Z T. Experiment and simulation on the incremental bend forming technology of the integral wing-skin panel. Metal Forming Technology 2003; 21(6): 23-25. [in Chinese]

[3] Liu J S, Zhang S H, Zeng Y S, et al. Simulation of incremental forming of integral panel skin with grid-type ribs. Materials Science and Technology 2004; 12(5): 515-517. [in Chinese]

[4] Liu J S, Zhang S H, Zeng Y S, et al. Finite element simulation of stress and strain on the incremental bend forming technology of the integral wing-skin panel. Journal of Plasticity Engineering 2003; 10(5): 42-45. [in Chinese]

[5] Ren L M, Wang Z T, Liu J S, et al. Analysis and numerical simulation on stability in irregular section of ribs bending process. Journal of Plasticity Engineering 2003; 10(5): 39-41. [in Chinese]

[6] Liu J S. Incremental forming and self-adapting control on integral panel skin with grid-type ribs. PhD thesis, Institute of Metal, Chinese Academy of Sience, 2004: 1-14. [in Chinese]

[7] Jiang N X, Liu J S, Zeng Y S. Research on the parameter forecasting of self-adapting incremental bending forming on integral panel skin with grid-type ribs. Transactions of Shenyang Ligong University 2006; 25(3): 15-18. [in Chinese]

[8] Liu J S, Zhang S H, Zeng Y S, et al. Determination of feature line equation for self-adapting incremental press bending. Journal of Materials Science and Technology 2004; 20(6): 739-742.

[9] Yue F L, Liu J S, Zhang S H, et al. Knowledge base research on the incremental press bending technology of integral wing-skin panel. Materials Science and Technology 2008; 16(3): 306-309. [in Chinese]

[10] Lee H W, Arunasalam P, Laratta W P. Neuro-genetic optimization of temperature control for a continuous flow polymerase chain reaction microdevice. Journal of Biomechanical Engineering 2007; 129(8): 540-547.

[11] Adineh V R, Aghanajafi C, Dehghan G H, et al. Opti-

mization of the operational parameters in a fast axial flow CW $CO_2$ laser using artificial neural networks and genetic algorithms. Optics & Laser Technology 2008; 40(8): 1000-1007.

[12] Zhang D, Zhang W H. Optimization of thermal stress and deformation of the casting during solidification by neural network and genetic algorithm. Acta Aeronautica et Astronautica Sinica 2006; 27(4): 697-702. [in Chinese]

[13] Jansson T, Nilsson L. Optimizing sheet metal forming processes—using a design hierarchy and response surface methodology. Journal of Materials Processing Technology 2006; 178(1-3): 218-233.

[14] Takayama K, Fujikawa M, Obata Y, et al. Neural network based optimization of drug formulations. Advanced Drug Delivery Reviews 2003; 55(9): 1217-1231.

[15] Mandal S, Sivaprasad P V, Venugopal S. Artificial neural network modeling of composition-process-property correlations in austenitic stainless steels. Materials Science and Engineering 2008; 485(1-2): 571-580.

[16] Sadeghi B H M. A BP-neural network predictor model for plastic injection molding process. Journal of Materials Processing Technology 2000; 103(3): 411-416.

[17] Xu Y M, Li S, Rong X M. Composite structural optimization by genetic algorithm and neural network response surface modeling. Chinese Journal of Aeronautics 2005; 18(4): 310-316.

[18] Al-Ahmari A M A. Predictive machinability models for a selected hard material in turning operations. Journal of Materials Processing Technology 2007; 190(1-3): 305-311.

[19] Shyy W, Tucker P K, Vaidyanathan R. Response surface and neural network techniques for rocket engine injector optimization. Journal of Propulsion and Power 2001; 17(2): 391-401.

[20] Pal S, Pal S K, Samantaray A K. Artificial neural network modeling of weld joint strength prediction of a pulsed metal insert gas welding process using arc signals. Journal of Materials Processing Technology 2008; 202(20): 464-474.

[21] Kurtaran H. A novel approach for the prediction of bend allowance in air bending and comparison with other methods. The International Journal of Advanced Manufacturing Technology 2008; 37(5-6): 486-495.

[22] Cheng J, Li Q S, Xiao R C. A new artificial neural network-based response surface method for structural reliability analysis. Probabilistic Engineering Mechanics 2008; 23(1): 51-63.

[23] Yan Y, Wan M, Wang H B. FEM equivalent model for press bend forming of aircraft integral panel. Transactions of Nonferrous Metals Society of China 2009; 19(2): 414-421.

[24] Fowlkes W Y, Creveling C M. Engineering methods for robust product design. Massachusetts, MA: Addison Wesley Longman Inc., 1995.

## Biography:

**Yan Yu** Born in 1983, she received B.S. degree from Yanshan University in 2005. Her main research interest lies in finite element simulation and optimization of metal forming processes.
E-mail: anneyan@126.com